Journal of Carcinogenesis
Covering Genesis to Therapeutics

Journal of Carcinogenesis, ISSN: 1477-3163
2025; Vol 24: Issue 3s, https://carcinogenesis.com/

Formulation and Evaluation of Magnetic Liposomal Aerosol Containing Etoposide in the treatment of Lung Cancer

Supriya Bhagwat[1a,1b], Dr.Vipul P.Patel[2]

[1a]Department of Pharmaceutics, Sanjivani College of Pharmaceutical Education and Research,Affiliated to Savitribai Phule Pune University, Ahilyanagar: 423601, Maharashtra, India.

[1b]Department of Pharmaceutics, School of Pharmaceutical Sciences, Sanjivani University, Kopargaon, Ahilyanagar: 423601, Maharashtra, India.

[2]Director and Professor, Sanjivani College of Pharmaceutical Education and Research,Affiliated to Savitribai Phule Pune University, Ahilyanagar: 423601, Maharashtra, India.

Corresponding Author: Supriya Bhagwat, Email Id: supriyasb511@gmail.com

Orchid Id: https://orcid.org/0009-0000-6261-7362

ABSTRACT

Lung cancer remains one of the leading causes of cancer-related mortality worldwide, largely due to late diagnosis, systemic toxicity of conventional chemotherapy, and the emergence of multidrug resistance. Etoposide, a topoisomerase II inhibitor, is widely used in treating small-cell lung carcinoma (SCLC); however, its clinical use is limited by poor aqueous solubility, rapid clearance, and non-specific distribution, leading to severe side effects. This study aims to develop and evaluate a magnetically guided liposomal drug delivery system encapsulating etoposide for targeted lung cancer therapy. Liposomes, due to their biocompatibility and ability to encapsulate both hydrophilic and hydrophobic drugs, were selected as the carrier system. Superparamagnetic iron oxide nanoparticles (SPIONs) were incorporated into the liposomes to enable magnetic field-guided targeting, improving drug localization at tumor sites. The prepared magnetic liposomes were characterized for particle size, surface charge, entrapment efficiency, morphology, and magnetic properties. In vitro release studies demonstrated sustained and controlled drug release, while cytotoxicity assays on A549 lung cancer cells showed enhanced anticancer activity compared to free etoposide. The presence of an external magnetic field significantly improved cellular uptake and localization. This targeted approach aims to overcome the pharmacokinetic limitations of etoposide, reduce systemic toxicity, and enhance therapeutic efficacy. The findings suggest that etoposide-loaded magnetic liposomes offer a promising non-invasive strategy for lung cancer treatment, warranting further preclinical and clinical evaluation.

Keywords: *Lung cancer, Novel drug delivery, magnetic nanoparticles, etoposide, liposome.*

How to Cite: Supriya Bhagwat, Dr.Vipul P.Patel, (2025) Formulation and Evaluation of Magnetic Liposomal Aerosol Containing Etoposide in the treatment of Lung Cancer, *Journal of Carcinogenesis, Vol.24, No.3s,* 523-539.

1. INTRODUCTION

Requirement for Targeted Drug Delivery Systems

Due to the shortcomings of traditional therapies, it is imperative to have targeted drug delivery systems capable of increasing the therapeutic index of anticancer drugs without increasing systemic toxicity. These systems propose to deliver the drugs directly to the tumor sites, thereby increasing local drug concentration and lowering healthy tissue exposure. One of the promising methods is the application of liposomes—lipid bilayer spherical vesicles—as drug carriers. Liposomes are capable of encapsulating hydrophilic and hydrophobic drugs, shielding them from degradation, and allowing controlled release [10]. Furthermore, surface modification of liposomes with targeting ligands or polyethylene glycol (PEG) can enhance their circulation time and specificity to tumor cells. The use of magnetic nanoparticles in liposomal formulations introduces another level of control. Targeting of the drug to the site is possible for magnetic liposomes by steering an external magnetic field to the cancer site for delivering medication. Beyond enhancing therapeutic agents' delivery to the cancer location, the scheme minimizes off-target effects via the systemically [11].

Etoposide and Its Limitations

Etoposide, a topoisomerase II inhibitor, is extensively used in the therapy of numerous malignancies, such as lung cancer. It acts by interfering with DNA replication, causing cell cycle arrest and apoptosis. Although highly effective, etoposide's therapeutic utility is compromised by poor solubility, high clearance, and extensive systemic toxicity [12]. These pharmacokinetic constraints require high doses, further increasing side effects . Encapsulation of etoposide in liposomal carriers, most notably magnetic liposomes, has the potential to circumvent these issues. They have the ability to increase the drug's solubility, prevent its premature degradation, and deliver it specifically to the site of the tumors, thus enhancing the therapeutic effects and limiting toxicity.

Etoposide's Role in Lung Cancer Therapy

Etoposide, a semisynthetic podophyllotoxin derivative, has emerged as a critical agent in the treatment of many cancers, such as small-cell lung cancer (SCLC) and non-small cell lung cancer (NSCLC). Initially, etoposide was isolated from the Podophyllum plant; etoposide functions mainly by inhibiting the activity of topoisomerase II, an enzyme essential for DNA replication and repair. The therapeutic effectiveness of etoposide is particularly pronounced in SCLC, where it has been theorized as an agent for first-line use when used with platinum chemotherapy like cisplatin or carboplatin. Such regimens are standard in extensive-stage SCLC, a type characterized by aggressive clinical course and early metastasis [13]. The efficacy of etoposide is largely attributed to its ability to produce DNA double-strand breaks and prevent the repair of breaks, which leads to cell death, primarily by apoptosis. The drug is typically used in combination with platinum-based chemotherapy regimens because platinum drugs induce DNA crosslinking and consequently enhance the ability of etoposide to induce DNA damage in cancer cells [14]. In non-small cell lung cancer, although etoposide is not a standard single-agent therapy, it is part of combined chemotherapy regimens, generally in combination with cisplatin, most commonly for the advanced disease or as a multimodality treatment. More recent studies have demonstrated that the addition of etoposide to new agents or other chemotherapy agents may enhance survival in some cases and decrease toxicity in NSCLC, although these combinations are less commonly used than in SCLC chemotherapy regimens [15].

Liposomes as Drug Carriers

Liposomes are artificially prepared vesicular structures composed of one or more concentric phospholipid bilayers, capable of encapsulating hydrophilic molecules in their aqueous core and hydrophobic drugs within the lipid bilayer. Since their discovery in the 1960s, liposomes have evolved into one of the most promising and biocompatible nanocarriers for drug delivery applications. Their ability to modulate the pharmacokinetics and pharmacodynamics of encapsulated drugs, improve drug stability, and reduce systemic toxicity has made them particularly attractive in cancer therapy. The basic architecture of liposomes includes amphipathic phospholipids that spontaneously form bilayered vesicles in aqueous environments. Cholesterol is frequently included in liposomal formulations to enhance membrane rigidity and stability. Furthermore, liposomes can be engineered to

possess specific characteristics—such as desired size, surface charge, lamellarity, and surface ligands—allowing them to meet the unique needs of different therapeutic interventions.[42]

2. DRUG PROFILE

Etoposide (ETP)

Etoposide is a semisynthetic derivative of podophyllotoxin, a cytotoxic compound derived from the *Podophyllum* plant. It is widely used as an antineoplastic agent and is classified as a topoisomerase II inhibitor. Etoposide exerts its anticancer effect by inducing DNA strand breaks during the DNA replication process, ultimately triggering apoptosis in rapidly dividing cancer cells. It is commonly used in the treatment of various malignancies, including small cell lung cancer, testicular cancer, lymphomas, and certain leukemias.

Appearance: White to off-white crystalline powder

IUPAC Name: (5R,5aR,8aR,9R)-5-(4,6-O-ethylidene-β-D-glucopyranosyl)oxy-9-(4-hydroxy-3,5-dimethoxyphenyl)5,8,8a,9tetrahydrofuro[3′,4′:6,7]naphtho[2,3d][1,3]dioxol-6(5aH)-one

Molecular Formula: C29H32O13

Chemical Structure:

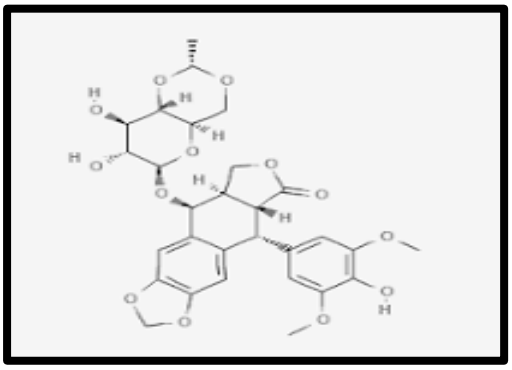

Fig. 1: Etoposide structure

Molecular Weight: 588.56 g/mol
Melting Point: 261–263°C (decomposes)
Half-life: 4–11 hours (dose and route dependent)
Log P: ~2.15
Protein Binding: Approximately 94% bound to plasma proteins, primarily albumin
pKa: ~10.6 (phenolic group)
Therapeutic Category: Antineoplastic agent (Topoisomerase II inhibitor)
Solubility: Poorly soluble in water; freely soluble in dimethylformamide, soluble in methanol and ethanol
Dose: Varies based on cancer type and regimen; typically 50–100 mg/m²/day for 5 days (IV or oral)
BCS Class: IV (Low solubility and low permeability)
Absorption: Oral bioavailability is approximately 25–75%; absorption may be incomplete and variable
Metabolism: Etoposide is metabolized primarily in the liver by the cytochrome P450 isoenzyme CYP3A4. A small amount undergoes O-demethylation and glucuronidation.
Excretion: Approximately 40–60% of the drug is excreted unchanged in the urine, and about 6% infeces.
Mechanism of Action: Etoposide acts by inhibiting DNA topoisomerase II, an enzyme involved in the unwinding of DNA for replication and transcription. The drug stabilizes the transient DNA double-strand breaks induced by topoisomerase II, thereby preventing relegation of the DNA strands. This leads to accumulation of DNA breaks, inhibition of DNA synthesis, and eventually apoptosis of cancer cells. Etoposide is most active in the late S and early G2 phases of the cell cycle.

3. MATERIAL AND METHODS

Materials

Table no. 1: Material used to formulate Magnetic Liposome

Sr. No.	Materials	Name of manufacturer
1	Etoposide	Moleculo Chem Pvt. Ltd.
2	Soya Phospholipid	Research Lab Fine Chem Industries, Mumbai, Maharashtra
3	cholesterol	Loba Chemie, Mumbai, Maharashtra
4	HPBCD	Modern Industries, Nashik, Maharashtra
5	Iron Oxide Nanoparticle	Research Lab Fine Chem Industries, Mumbai, Maharashtra
6	Ethanol	Loba Chemie, Mumbai, Maharashtra
7	Chloroform	Research Lab Fine Chem Industries, Mumbai, Maharashtra
8	Methanol	Research Lab Fine Chem Industries, Mumbai, Maharashtra
9	Sodium Hydroxide	Research Lab Fine Chem Industries, Mumbai, Maharashtra
10	Potassium Dihydrogen Phosphate	Research Lab Fine Chem Industries, Mumbai, Maharashtra
11	HPLC Water	Finar limited, Ahmedabad, Gujrat

Table no. 2: List of Instruments

Sr. No	Instruments	Name of Manufacturer
1	Electronic Digital Balance AY 120	Shimadzu
2	Magnetic Stirrer	Remi equipment Pvt. Ltd, Mumbai India
3	UV Visible Spectrophotometer	Shimadzu UV 1800
4	Ultrasonicator	PCI Analytics
5	Rotary Evaporator	Orchid Scientific Buchi
6	Centrifuge	Remi CL 24
7	DSC	Brookfield
8	Microplate Reader	Thermoscientific
9	FTIR Spectrophotometer	Shimadzu 8400s
10	Microtrac Nano Particle Analyzer	Nanotrac Wave-II
11	pH meter	Lab India

Methods

A) Pre-formulation study of pure drug Etoposide

a) Melting point (MP)

The MP of etoposide was determined by using digital melting point apparatus. For determination of MP drug was taken in a glass capillary whose one end was sealed by flame. The capillary-containing drug was dipped in liquid paraffin inside the MP which was equipped with a magnetic stirring facility. DSC was also used for melting point determination.

b) Differential Scanning Calorimetry (DSC)

Differential scanning calorimetry (DSC–60 SHIMADZU) measurement was performed by a thermal analyzer. Thermally sealed 5mg sample weighed in an aluminum pan Conditions such as a heating rate of 10°C/min from 0 to 300°C for scanning with a drynitrogen flush at a rate of 30ml/min are used to obtain thermograms. the thermal properties of the pure drug were characterized**.**[63]

c) Calibration curve of UV visible spectroscopy

10 mg etoposide was weighed accurately and transferred in a 100 ml volumetric flask containing phosphate buffer pH 7.4. Prepare a stock solution of 100 µg/ml and kept the stock solution for the sonication for 15 min. Preparations of dilutions from a stock solution of etoposide concentrations of 8, 10, 12, 14, 16 and 18 µg/ml prepared from a stock solution of 100 µg/ml. Standard calibration curve of etoposide plotted with the absorbance of etoposide solution in a concentration range of 8-18 µg/ml at 285 nm using UV-visible spectrophotometer. etoposide concentration was plotted on the X-axis and absorbance on the Y-axis.[64]

d) FTIR Analysis

The FTIR study of the drugs was carried out to identify the functional group.
Samples of FTIR:
Sample A: Etoposide pure drug
Sample B: Etoposide + SPC
Sample C: Etoposide + HPBCD
Sample D: Etoposide + Cholesterol
Sample E: Etoposide + MNP

e) Compatibility evaluation using FTIR

To provide the optimum interaction, the drug and excipient ratio in the formulation of magnetic liposome was studied at a 1:1 proportion. Additionally, the interaction between the drug and excipient was verified by FTIR (Shimadzu 8400s) in the scanning range of 4000– 400 cm^{-1}.[65]

B) Experimental designs

Magnetic Liposome formulations underwent optimization through a 32 Central Composite design, involving 9 experiments. Design of Experiment (DOE) was constructed utilizing Design expert v. 13. The dependent variable was selected are concentration of soya phosphatidylcholine and Cholesterol (Table. 3) to analyze the effect on Particle Size, entrapment Efficiency and Zeta Potential of Magnetic Liposome batches. Table 3 Experimental design independent factor Level +1 0 -1 Soya phosphatidylcholine concentration 300 - 500 Cholesterol concentration 75 - 125 Formulation of Magnetic Liposome Batches.

Table 3: Level used in experimental design

Factors	Levels used			Values added		
	Low	Medium	High	Low	Medium	High
Soya Phospholipid conc.	-1	0	+1	300	400	500
Cholesterol conc.	-1	0	+1	75	100	125

Fig.no.2: Formulation of Etoposide loaded Magnetic Liposome

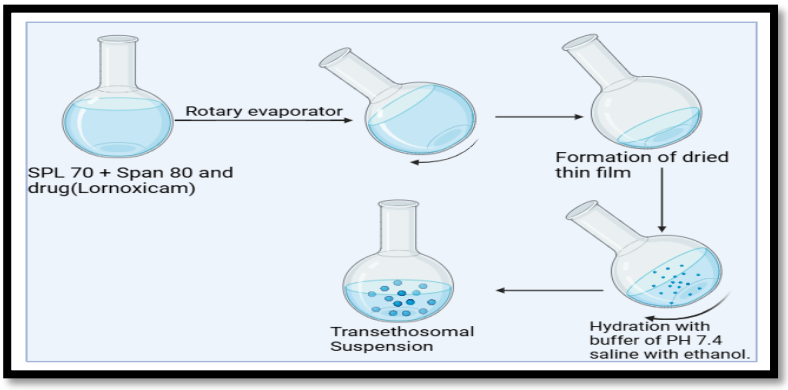

Etoposide-loaded liposomes were prepared using the thin-film hydration method with Soya phosphatidylcholine and cholesterol (4:1 ratio), keeping the drug amount constant. Etoposide (10 mg), cholesterol, phosphatidylcholine, and iron oxide nanoparticles were dissolved in 10 mL chloroform in a round-bottom flask. The solvent was evaporated at 40°C under vacuum (100 rpm, 30 min) to form a thin film, which was then left overnight and hydrated with 10 mL phosphate buffer (pH 7.4) at 30°C for 1 hour. The dispersion was sonicated (30 and 60 min) to ensure homogeneity and centrifuged at 10,000 rpm for 60 minutes. [66]

The formulations were stored at 4°C until further analysis.

Fig. 3: Dried thin film

E) Magnetic Liposome Characterization

a) Particle size and zeta potential

The Microtrac MRB zeta sizer was used to measure particle size, PDI, and zeta potential of etoposide-loaded magnetic liposomes. Samples were diluted 1:10 with distilled water for proper scattering. Dynamic Light Scattering (DLS) assessed particle size based on Brownian motion, while zeta potential measured surface charge and colloidal stability. A high absolute zeta potential (±30 mV or more) indicates strong stability, which helps predict aggregation and biological interactions.

b) Drug Entrapment efficiency

Entrapment efficiency was determined by ultracentrifugation. Two mL of each formulation was centrifuged at 15,000 rpm for 60 minutes at 4°C to separate free drug from liposomes. The liposomal pellets were washed with PBS (pH 7.4) and centrifuged again. The combined supernatant was diluted and analyzed at 285 nm using a UV spectrophotometer to quantify the free drug.

c) Scanning Electron Microscopy (SEM)

The SEM is one of the most limited instruments widely applied to surface microstructure imaging. SEM is a type of electron microscopy that images the sample surface of a solid specimen by using a focused beam of high-energy electrons. Liposomes were characterized by SEM. SEM analysis provides information related to microstructure, morphology, and topographical and elemental evidence of nanomaterials. SEM analysis was used to determine the surface morphology of the etoposide loaded magnetic liposome.

d) Magnetic Property check

The magnetic properties of magnetic liposomes can be evaluated using Vibrating Sample Magnetometry (VSM), which provides a magnetization curve indicating super paramagnetic behaviour through parameters like saturation magnetization and coercivity. A magnetic separation test offers a quick qualitative check, where liposomes are attracted to a magnet, confirming magnetic responsiveness. Transmission Electron Microscopy (TEM) can visualize the iron oxide core within the liposome structure. Dynamic Light Scattering (DLS) can show aggregation changes under a magnetic field. For therapeutic applications, magnetic hyperthermia testing assesses heat generation under an alternating magnetic field, confirming functional magnetic performance.

e) MTT assay

The cytotoxic effects of compounds were tested in vitro using an MTT assay

Step-1 Overnight, 100 µL of DMEM-medium was used to seed cells at a density of 1×106 cells/well in 96-well plates.

Step-2 Cells were then treated with different concentrations of the compounds for 24 h.

Step-3 Following a 24-hour treatment, each well received 20 µL of MTT reagent, and the plates were subsequently incubated for 4 hours at 37°C.

Step-4 The medium containing MTT was aspirated and the formazan crystals were solubilized by the addition of 100 µL DMSO.

Step 5 With the aid of an ELISA microplate reader (Thermo, USA), the absorbance of colored formazan products was measured between 570 and 600 nm. The negative control was DMSO at a concentration of 0.1%, and the positive reference standards were methotrexate. The GraphPad Prism program was used to create the dose-response curve. The same program was used to calculate the concentration of each drug that resulted in a 50% growth inhibition as well as the associated 95% confidence interval. The following formula was used to fit the dose-response curve and determine the percentage viability.). [69].

% of Inhibition = Control OD – Sample OD / Control OD × 100

Cytotoxicity assay (normal cell line):

To find out how harmful a substance is to healthy cells, an experiment was carried out. Two different cell lines were employed for this: the HEK-293 (human embryonic kidney cell), both of which were acquired from the National Centre for Cell Science, Pune (NCCS). The test's methodology was comparable to that of the MTT assay, which evaluates cell viability.

Step-1 Cells were first seeded at a density of 1 × 10^3 cells/mL into each well of a 96-well plate, and they were then incubated for 24 hours at 37°C with 5% CO2. A phytochemical and a conventional medication were then administered to the cells at a dosage of 1 mg/1 mL DMSO (dimethyl-sulfoxide). Following serial dilution treatment, the cells were cultured for 24 hours at 37°C in a CO2 incubator.

Step-2 After a day, MTT dye (MTT, which stands for 3-(4,5-dimethylthiazol-2-yl)-2,5-diphenyl tetrazolium bromide) was used to evaluate the phytochemical compound's cytotoxicity. Each well received 20 ul of MTT dye, and the plate was incubated for three hours at 37°C with 5% CO2.

Step-3 Within the cells, yellow formazan crystals developed after three hours. Following the removal of 50 ul of MTT dye from each well, 100 ul of DMSO solution was added in order to dissolve the crystals. A Skanlt microplate reader was used to measure the absorbance at 570 nm after the plates were shaken for five minutes at 900 rpm on a microplate orbital shaker (LabDoctor from MidSci, St. Louis, MO [7], [8].

4. RESULT AND DISCUSSION

Preformulaion Study

Identification and confirmation of drug Etoposide

The drug was confirmed using UV spectroscopy, FTIR spectroscopy.

a) Calibration curve of UV Visible spectroscopy

The analysis was carried out in between the range of 400 nm-200 nm. The obtained results were in the ideal range reported in the referred literature survey. The ranges and their outcomes are shown in Fig. 9.

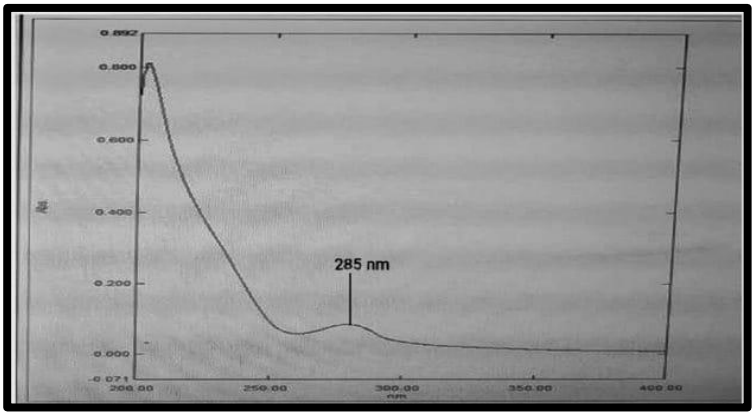

Fig.4: UV spectra of Etoposide

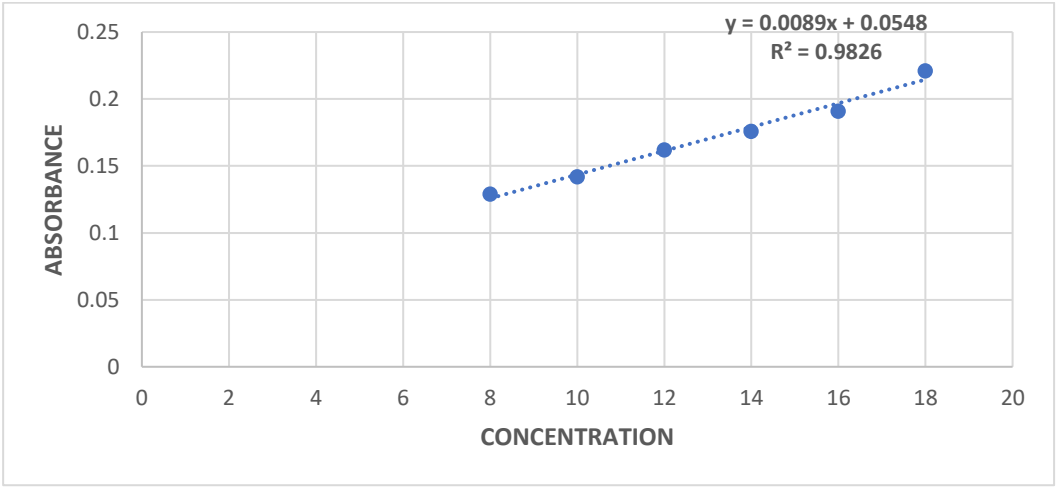

Fig.5: Calibration curveofpuredrugEtoposideinphosphatebufferpH7.4

Table no 4: Standard calibration curve of PAC in phosphate buffer pH 7.4

Conc. (ppm)	Absorbance			Mean	SD
	A1	A2	A3		
0	0	0	0	0	0
8	0.090	0.093	0.0.094	0.092	±0.002
10	0.121	0.125	0.126	0.124	±0.003
12	0.145	0.148	0.147	0.147	±0.002
14	0.174	0.176	0.175	0.175	±0.001
16	0.190	0.195	0.197	0.194	±0.004
18	0.205	0.209	0.8	0.208	±0.003

FTIR Analysis

The spectrum of pure etoposide presented characteristic peaks at 3400–3200 cm^{-1} (broad O–H stretching, due to phenolic and alcoholic hydroxyl groups), 2940–2830 cm^{-1} (C–H stretching of aliphatic $–CH_2$ groups), 1760–1720 cm^{-1} (strong C=O

stretching for the lactone carbonyl group), 1600–1450 cm^{-1} (aromatic C=C stretching), 1250–1000 cm^{-1} (C–O–C stretching in the methoxy and glycosidic bonds), and around 830–750 cm^{-1} (aromatic C–H bending). These peaks clearly indicate that etoposide shows compatibility with the excipients used in magnetic liposomes.

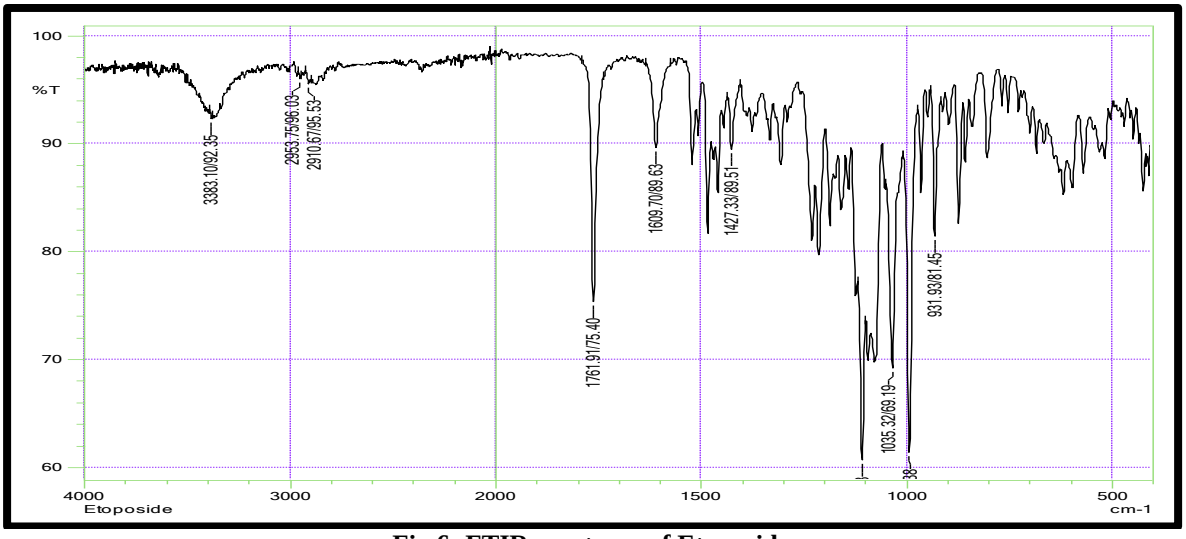

Fig.6: FTIR spectrum of Etoposide

Compatibility evaluation using FTIR

The physical mixture of etoposide, Soya phosphatidylcholine cholesterol, HPBCD, MNP and all excipients was analyzed, the characteristic peaks of drugs were present in the physical mixture similar to that of an individual drug spectrum, and there were no discernable changes in FTIR spectra, which confirmed the absence of any chemical interactions between them as shown in Fig. 12. The thermogram of Etoposide showed characteristics typical of a crystalline substance, displaying an endothermic peak at 275 °C due to melting, followed by an exothermic peak at 294 °C (Fig. 5), which was due to its decomposition and is associated with the crystallization of the drug.

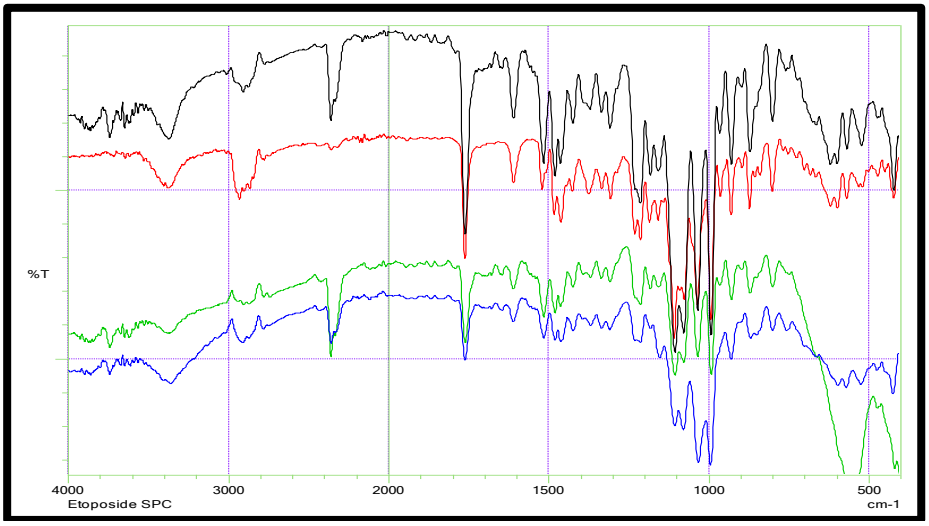

Fig.7: FTIR optimized Drug excipients compatibility study

	SOYAPHOSPHATIDYLCHOLINE + ETOPOSIDE
	CHOLESTEROL + ETOPOSIDE
	HPBCD + ETOPOSIDE
	MNP + ETOPOSIDE

Table no. 5: Colour marking indicates Compatibility study

Differential Scanning Calorimetry

The thermogram of Etoposide showed characteristics typical of a crystalline substance, displaying an endothermic peak at 275 °C due to melting, followed by an exothermic peak at 294 °C (Fig. 14), which was due to its decomposition and is associated with the crystallization of the drug.

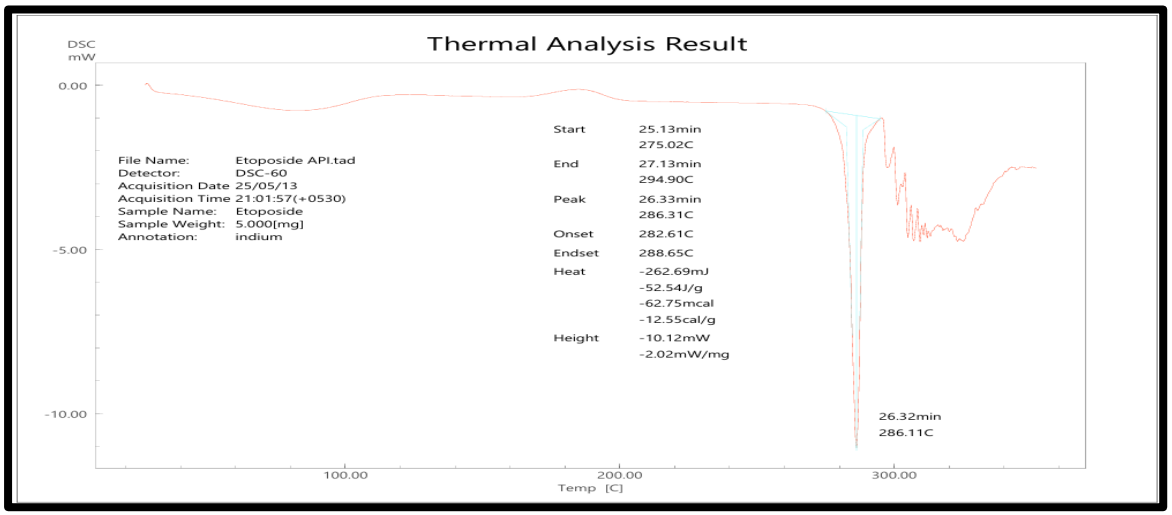

Fig. 8: DSC of pure etoposide

Optimization of Liposomal formulation by using design 2^3 Central Composite Design

For the optimization of etoposide loaded Magnetic Liposome central composite design was used. The independent variables were cholesterol concentration (X1), soya phosphatidylcholine (X2), entrapment efficiency (Y1), particle size (Y2), and zetapotential (Y3), were taken as dependent variables.

Table No. 6 Optimization of Liposomal formulation by using regular two-level factorial design 2^3

Run	Soya phosphatidylcholine (mg)	Cholesterol (mg)	Particle Size (nm)	Zeta Potential (MV)	Entrapment Efficiency (%)
1	500	75	127	-32	58.8
2	500	100	175	-36	66.1
3	400	100	205	-35	68
4	500	125	147	-25	65
5	300	75	152	-28	65.55
6	400	125	130	-24	61
7	300	100	121	-14	56
8	400	75	118	-18	59.7
9	300	125	124	-23	67.1

Effect on Particle Size

The 3D Surface plot illustrates the influence Soya phosphatidyline of & cholesterol Concentrations of levels increase the Particle Size also Ranging from approximately 100 to 220 nm.

The lowest Particle size were observed at The lower Concentration Components, while Highest Sizes occurred that Higher lipid Content leades to the formation of larger liposome Possibly due to increased bilayer rigidity & Vesicle fusion.

Graph Show

As soya phosphatidylcholine Particle Size also increase cholesterol increased Highest Particle Size (220 cm) is observed of both at upper levels both Soya phosphatidylcholine and Cholesterol. The Smaller Particle Size occurs at lower level of Both SOYA phosphatidyline & cholesterol

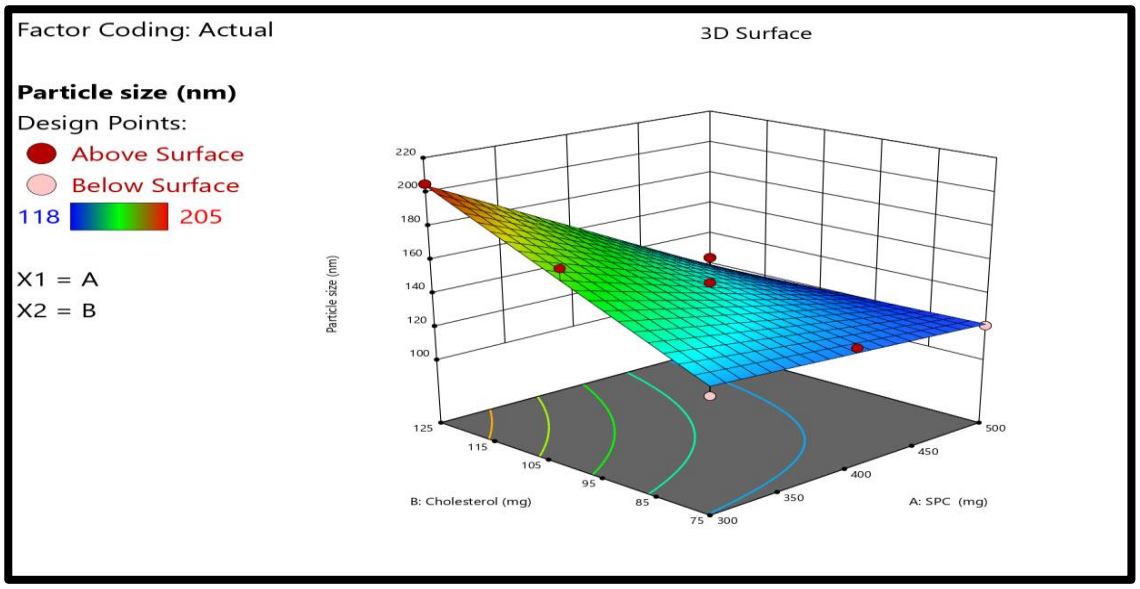

Figure No. 9: Surface 3D plot of particle size

ANOVA for 2FI model
Response 1: Particle size

Table no. 7 ANOVA for 2FI model [for Particle size]

Source	Sum of Squares	df	Mean Square	F-value	p-value	
Model	6630.42	3	2210.14	51.74	0.0003	significant
Soya phosphatidylcholine	3456.00	1	3456.00	80.91	0.0003	
B-Cholesterol	1768.17	1	1768.17	41.39	0.0013	
AB	1406.25	1	1406.25	32.92	0.0023	
Residual	213.58	5	42.72			
Cor Total	6844.00	8				

Factor coding is **Coded**.
Sum of squares is **Type III - Partial**

The **Model F-value** of 51.74 implies the model is significant. There is only a 0.03% chance that an F-value this large could occur due to noise.

P-values less than 0.0500 indicate model terms are significant. In this case A, B, AB are significant model terms. Values greater than 0.1000 indicate the model terms are not significant. If there are many insignificant model terms (not counting those required to support hierarchy), model reduction may improve your model.

Response 2: Effect on ZP

The 3D Surface Plot shows the effect of Soya phosphatidylcholine & cholesterol Concentration on Zeto Potential of the liposomal formulation as Both soya phosphatidylcholine + cholesterol level Increase Zeta Potential Becomes more negative ranging from Approximately -10 MV to -35 MV This indicates improved Conoidos Slobility Due to enhanced electrostatic Repulsion. The increased between soya phosphatidylcholine & cholesterol Significanly influences Zeta potential. Suggesting that Higher Concentration of both Components Contribute to more Stable liposome.

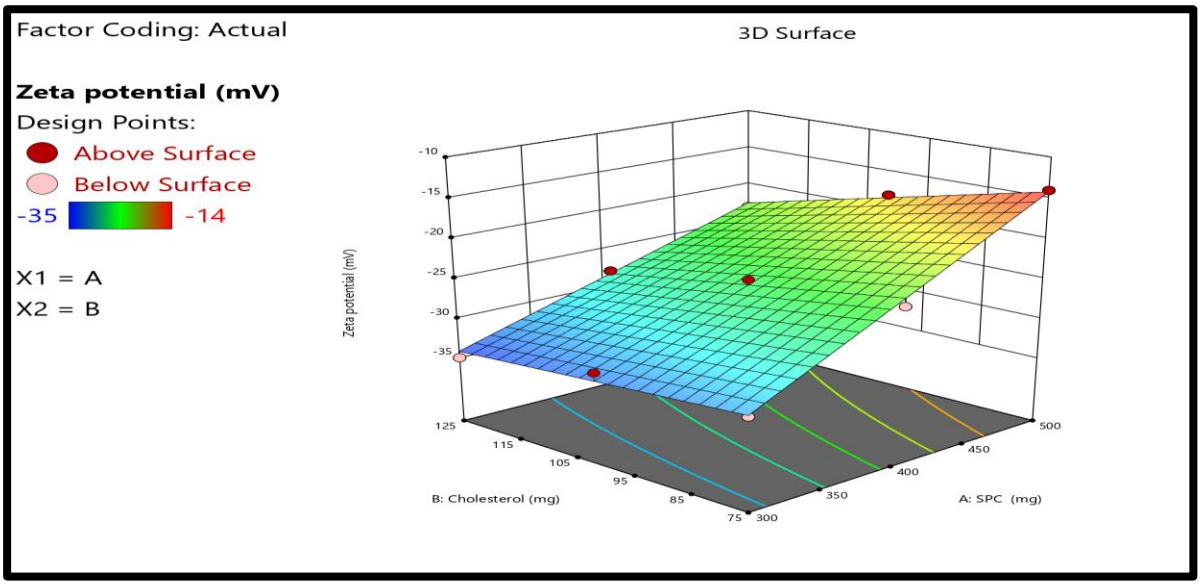

Figure No. 10: Surface 3D plot of zeta potential

ANOVA for 2FI model
Response 2: Zeta potential

Table no. 8 ANOVA for 2FI model [for zeta potential]

Source	**Sum of Squares**	**df**	**Mean Square**	**F-value**	**p-value**	
Model	374.33	3	124.78	170.15	< 0.0001	significant
Soya phosphatidylcholine	322.67	1	322.67	440.00	< 0.0001	
B-Cholesterol	42.67	1	42.67	58.18	0.0006	
AB	9.00	1	9.00	12.27	0.0172	
Residual	3.67	5	0.7333			
Cor Total	378.00	8				

Factor coding is **Coded**.
Sum of squares is **Type III - Partial**
The **Model F-value** of 170.15 implies the model is significant. There is only a 0.01% chance that an F-value this large could occur due to noise.

P-values less than 0.0500 indicate model terms are significant. In this case A, B, AB are significant model terms. Values greater than 0.1000 indicate the model terms are not significant. If there are many insignificant model terms (not counting those required to support hierarchy), model reduction may improve model.

Effect on Entrapment Efficiency

The 3D Surface Plot demonstrates the impact of soya phosphatidylcholine & Cholesterol concentrations on the of liposome EE of liposome formulation. EE increase with higher Cholesterol levels and decrease with increasing Soya phosphatidylcholeline concentration The Highest EE 68-70% was observed at low soya phosphatidylcholine & high Cholesterollevel while lower EE Occurred at high Soya phosphatidylcholeline & low Cholesterol. This suggests that Cholesterolenhances bilyer packing improving drug encapsulation.

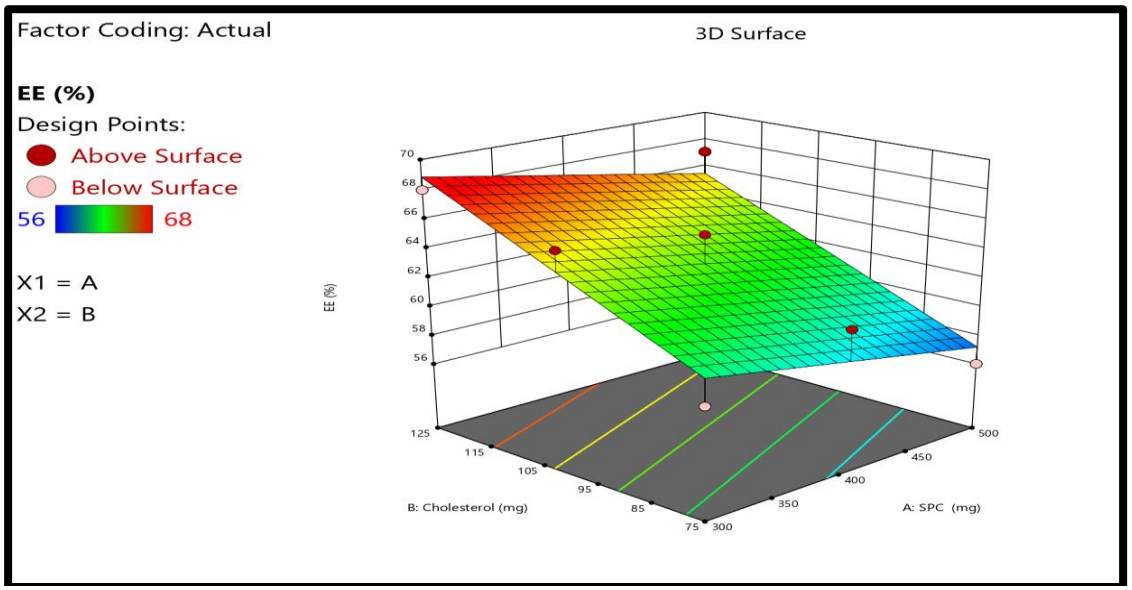

Figure no 11: Surface 3D plot of EE

ANOVA for Linear model
Response 3: EE

Table no. 9 ANOVA for 2FI model [for EE]

Source	Sum of Squares	df	Mean Square	F-value	p-value	
Model	119.92	2	59.96	15.29	0.0044	significant
A-Soya Phosphatidylcholine	17.00	1	17.00	4.34	0.0825	
B-Cholesterol	102.92	1	102.92	26.25	0.0022	
Residual	23.52	6	3.92			
Cor Total	143.45	8				

Factor coding is **Coded**.
Sum of squares is **Type III – Partial**

The **Model F-value** of 15.29 implies the model is significant. There is only a 0.44% chance that an F-value this large could occur due to noise.

P-values less than 0.0500 indicate model terms are significant. In this case B is a significant model term. Values greater than 0.1000 indicate the model terms are not significant. If there are many insignificant model terms (not counting those required to support hierarchy), model reduction may improve your model.

Characterization of Liposome

Particle Size and PDI

The table 5 and fig. 22 demonstrate the particle size values of the formed etoposide loaded magnetic liposome. The Particle Size values were between 100 nm and 220 nm. The PDI of the formulation was found to be 0.2 to 0.5. The PDI 0.3 indicates that the distribution consisted of a single size mode without showing aggregates. The size ranges for liposome according to the vesicular types are Based on the vesicle size, liposome can be divided into three groups.

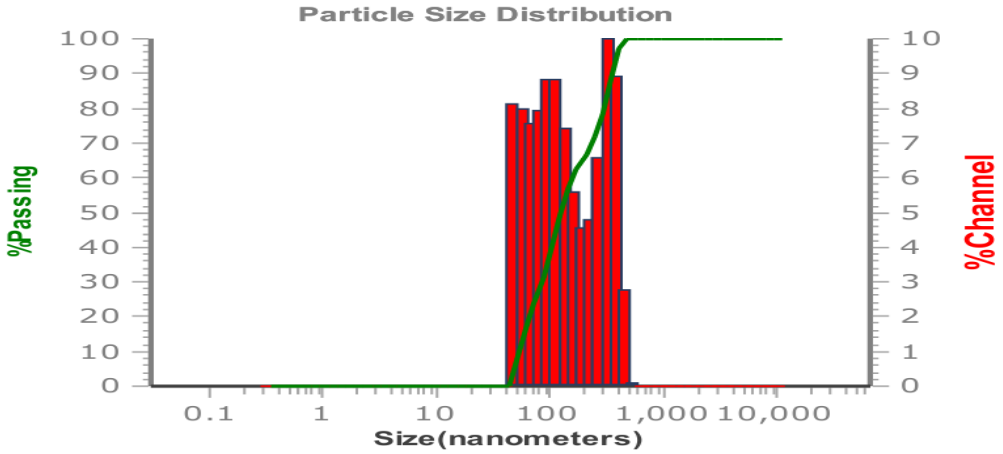

Fig. 12: Particle size distribution of liposome

Zeta Potential

The zeta potential between −10 and -35 mV are considered approximately neutral, while nanoparticles with zeta potentials ofgreater than +30 mV or less than −30 mV are considered strongly cationic and anionic, respectively. The Zeta Potentialof etoposideloadedliposomeoptimizedbatchwas-25.3mVindicatingthat the produced liposome had enough negative charge to sustain electric repulsion and limit aggregation, resulting in improved stability.

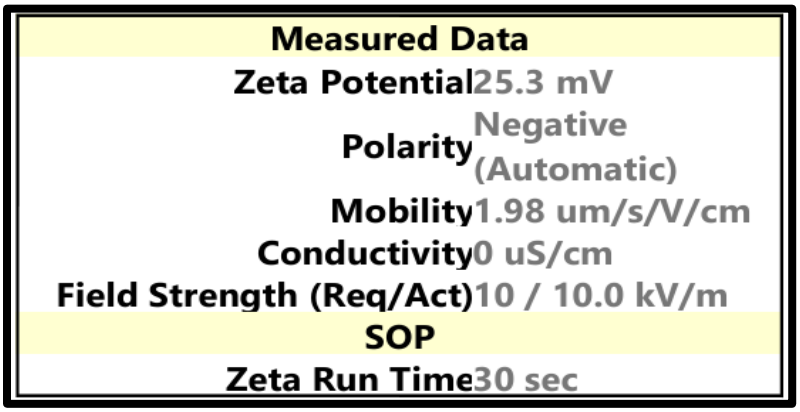

Fig. 13: Zeta potential of optimized batch

Scanning Electron Microscopy (SEM)

Study of SEM of optimized liposomal dispersion of showed that liposome produced spherical shape and morphology of vesicles of size range 100-119 µm.

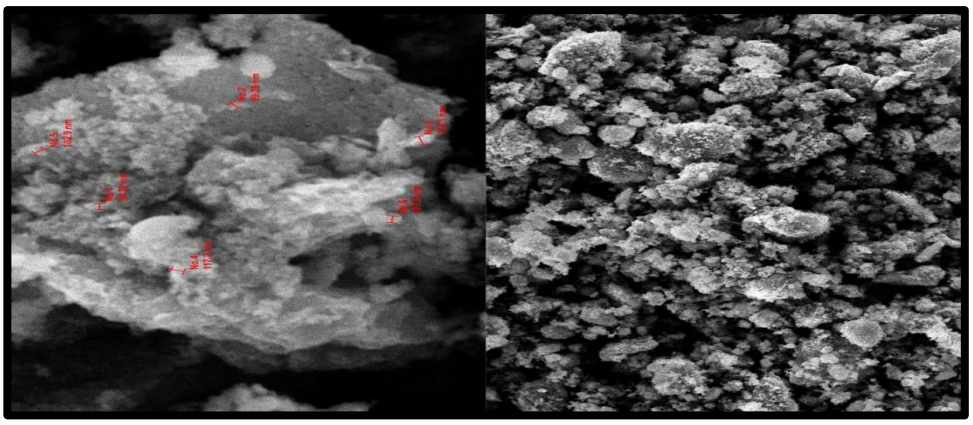

Fig. 14: SEM analysis of liposome

MTT Assay

The main aim of the MTT assay was to investigate the effect of etoposide on the cell viability using the lung cancer cell line (A549). It was incubated for 24 hrs. As mentioned in Figure 10 sample A was the optimized formulation and sample B was the etoposide. The IC50 value of A and B was found to be 101.6 and 308.3 (Table 10) respectively. It was calculated with the help of Graph Pad prism programmer (ver.5.04) (Graph Pad Software, Inc. USA)

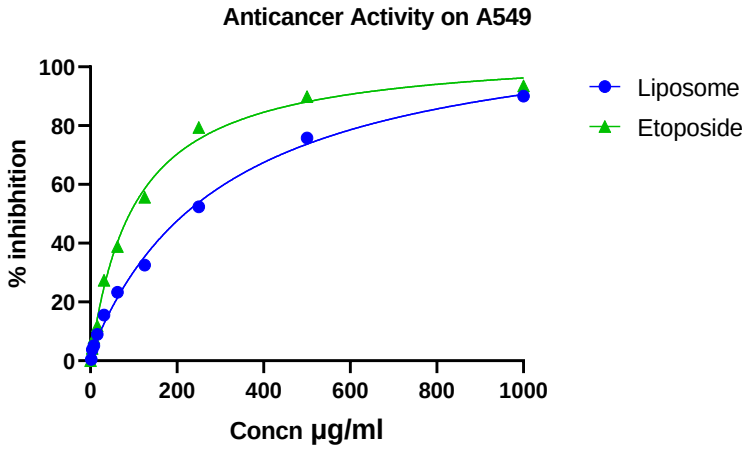

Fig no 15: IC 50 graph of Liposome and Etoposide

Table no 10: Observed % inhibition of etoposide and liposome on A549 Cytotoxicity on HEK-293 Cell line

Concentration	Etoposide	Liposome
1000	93.5181	90.0164
500	89.8337	75.7698
250	79.38	52.3923
125	55.6099	32.5059
62.5	38.8609	23.2994
31.25	27.4093	15.5581
15.63	11.8674	8.9458
7.81	7.7948	5.0973
3.91	4.2389	3.7598
1.95	2.4823	0.432
IC50	**101.6**	**308.3**

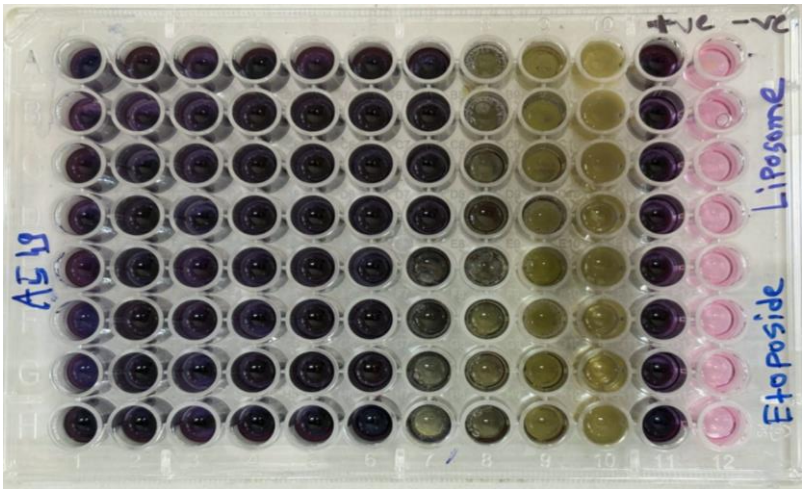

Fig. no. 16: Anticancer Activity on A549 Lung cancer cell line

The cytotoxic potential of the liposomal formulation was evaluated using an in vitro MTT assay across a wide concentration range (9.76–5000 µg/mL) against the selected cancer cell line. The results revealed a clear dose-dependent cytotoxic effect, wherein higher concentrations of the liposomal formulation induced greater cell death. At the maximum tested concentration (5000 µg/mL), the formulation exhibited approximately 47.5% cytotoxicity, whereas at the lowest concentration (9.76 µg/mL), only 2.06% cell death was observed. The half-maximal inhibitory concentration (IC_{50}) was calculated to be approximately 1215 µg/mL, indicating moderate cytotoxic activity. The relatively high IC_{50} value suggests that while the liposomal carrier system is capable of delivering the drug to the cells and inducing cytotoxic effects, further optimization may be required to enhance its therapeutic efficacy, possibly through improved drug loading, surface modification, or co-delivery strategies.

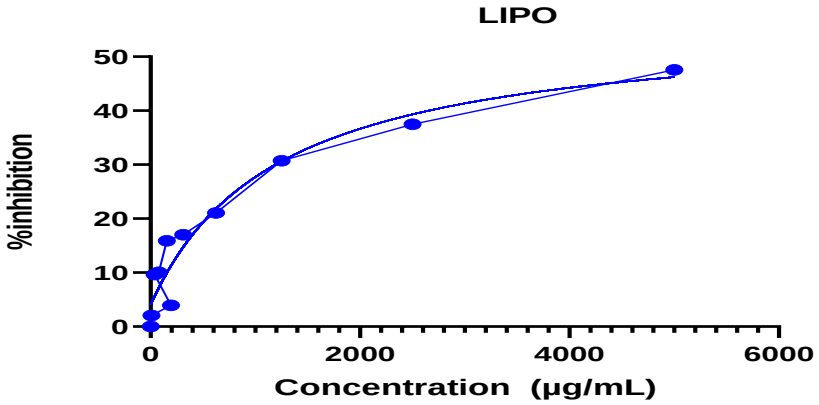

Fig. no 17: IC 50 value graph on HEK 293 cell lin

Fig. no18: Cytotoxicity on HEK-293 cell line

Table no 11: IC 50 value on HEK 293 cell line

Concentration (µg/mL)	LIPOSOME
1000	47.5438
500	37.4589
250	30.7132
125	21.065
62.5	17.0376
31.25	15.8974
15.63	10.048
7.81	9.645
3.91	3.9486
1.95	2.057
IC50	**1215**

5. SUMMARY AND CONCLUSION

The creation of a magnetic liposome formulation loaded with etoposides offers a viable strategy for the targeted treatment of non-small cell lung cancer (NSCLC). Based on important quality parameters such particle size, zeta potential, and entrapment efficiency, the study optimized two important formulation variables—soya phosphatidylcholine and cholesterol—using a 3^2 central composite design. During nine experimental runs, it was shown that while higher phosphatidylcholine concentrations resulted in an increase in particle size, higher cholesterol levels enhanced entrapment efficiency, reaching up to 70%. With a p-value below 0.05, the ANOVA analysis validated the optimization model by

confirming the considerable impact of cholesterol on the formulation's efficiency. Fourier Transform Infrared Spectroscopy (FTIR) and Differential Scanning Calorimetry (DSC) were used to verify the physicochemical compatibility of etoposide with the liposomal matrix. The prominent endothermic peak of pure etoposide vanished from the drug-loaded liposomes' DSC thermograms, indicating a change to a less crystalline or amorphous form—a beneficial alteration that improves the solubility of poorly soluble medications. Additionally, FTIR research confirmed the chemical stability and compatibility of the excipients with the medicine by demonstrating that the distinctive peaks of etoposide did not change in the final formulation, indicating no major interaction or chemical degradation. Liposomes' spherical and smooth form was shown by scanning electron microscopy (SEM), with particle sizes ranging from 100 to 119 µm. This was consistent with findings from dynamic light scattering (DLS), which showed particle sizes between 100 and 220 nm. High physical stability was shown by the lack of cracks or agglomeration, and good colloidal stability—which is necessary for long-term storage and consistent pulmonary delivery—was supported by a zeta potential of −25.3mV. The liposomal formulation demonstrated less anticancer activity than free etoposide, with an IC_{50} value of 101.6 µg/mL for etoposide , compared to 308.3 µg/mL for the free medication, according to an in vitro biological evaluation utilizing the MTT assay on A549 lung cancer cells. Additionally, the cytotoxicity profile showed dose-dependency, indicating consistent pharmacological action. An IC_{50} of 1215 µg/mL was found in investigations on HEK-293 normal cells, which is significant since it indicates selective toxicity toward cancer cells, which is essential for reducing side effects and enhancingpatient safety. The formulation's use of magnetic iron oxide nanoparticles was one of its unique features. When subjected to an external magnetic field, they improved site-specific delivery to lung cancers by enabling magnetically guided medication targeting. In addition to improving localized drug accumulation, this creates new opportunities for magnetic hyperthermia in the future, where local heating can aid in tumor elimination and accelerate drug release. A multipurpose, targeted drug delivery method that overcomes the drawbacks of traditional chemotherapy, including its poor solubility, limited bioavailability, and non-specific toxicity, is provided by the improved etoposide-loaded magnetic liposome formulation. As demonstrated by extensive in vitro testing and analytical evaluation, the formulation's excellent entrapment efficiency, stable physicochemical characteristics, and selective cytotoxicity were all attained by methodical optimization. The medication was successfully encapsulated within the lipid bilayer in a stable, amorphous state without sacrificing its molecular integrity, according to characterization experiments conducted using DSC, FTIR, and SEM. The liposomal formulation's physical robustness and high stability were demonstrated by its homogeneous shape and suitable surface charge. The system's therapeutic precision is demonstrated by its enhanced cytotoxic effect on cancer cells and low toxicity to healthy cells. A crucial innovation that improves spatial drug delivery and lessens off-target effects is externally guided targeting, which is made possible by the integration of IONs. In conclusion, this study offers a new and effective nanocarrier method for the delivery of etoposides in NSCLC. The study establishes the foundation for future in vivo research, pharmacokinetic analyses, and clinical translation in addition to proving the viability and advantages of magnetic liposome technology for lung cancer treatment. This strategy could revolutionize cancer treatment by fusing smart nanotechnology with traditional chemotherapeutics, making it safer, more effective, and more patient-friendly.

ACKNOWLEDGEMENT

The authors express gratitude to the Department of Science & Technology (DIST-FIST), New Delhi, Rajiv Gandhi Science & Technology Commission (RGSTC), Mumbai, and AICTE (MODROB) for their financial support in providing the central instrumentation facility at our college. All the authors are thankful to the management of SRES, Sanjivani College of Pharmaceutical Education and Research (Autonomous), Kopargaon, India, and School of Pharmaceutical Sciences, Sanjivani university ,Kopargaon, for providing the necessary facilities for the completion of this research work.

Conflict of Interest Declared None

REFERENCES

[1] X. Wang *et al.*, “Spatial relationship of tertiary lymphoid structures and tumor-associated neutrophils in bladder cancer and prognostic potential for anti-PD-L1 immunotherapy,” 2024. doi: 10.1002/cac2.12491.

[2] C. Li *et al.*, “Global burden and trends of lung cancer incidence and mortality,” *Chin Med J (Engl)*, vol. 136, no. 13, 2023, doi: 10.1097/CM9.0000000000002529.

[3] M. G. Sholih*et al.*, “Risk factors of lung cancer in Indonesia: A qualitative study,” *Journal of Advanced Pharmacy Education and Research*, vol. 9, no. 2, 2019.

[4] M. Mustafa, AR. J. Azizi, EL. IIIzam, A. Nazirah, S. Sharifa, and SA. Abbas, “Lung Cancer: Risk Factors, Management, And Prognosis,” *IOSR Journal of Dental and Medical Sciences*, vol. 15, no. 10, 2016, doi: 10.9790/0853-15100494101.

[5] M. C. Turner *et al.*, “Outdoor air pollution and cancer: An overview of the current evidence and public health recommendations,” *CA Cancer J Clin*, vol. 70, no. 6, 2020, doi: 10.3322/caac.21632.

[6] K. Zarogoulidis*et al.*, “Treatment of non-small cell lung cancer (NSCLC),” 2013. doi: 10.3978/j.issn.2072-1439.2013.07.10.

[7] M. P. Mansukhani, V. K. Somers, and S. M. Caples, “COUNTERPOINT: Should All Patients With Atrial

Fibrillation Who Are About to Undergo Pulmonary Vein Ablation Be Evaluated for OSA? No," 2018. doi: 10.1016/j.chest.2018.06.041.

[8] A. M. Hopkins, G. Kichenadasse, R. A. McKinnon, A. Rowland, and M. J. Sorich, "Baseline tumor size and survival outcomes in lung cancer patients treated with immune checkpoint inhibitors," *Semin Oncol*, vol. 46, no. 4–5, 2019, doi: 10.1053/j.seminoncol.2019.10.002.

[9] R. S. Herbst, D. Morgensztern, and C. Boshoff, "The biology and management of non-small cell lung cancer," 2018. doi: 10.1038/nature25183.

[10] D. D. Lasic, "Mixed micelles in drug delivery," 1992. doi: 10.1038/355279a0.

[11] S. Fathi and A. K. Oyelere, "Liposomal drug delivery systems for targeted cancer therapy: Is active targeting the best choice?," 2016. doi: 10.4155/fmc-2016-0135.

[12] F. Zare Kazemabadi, A. Heydarinasab, A. Akbarzadeh, and M. Ardjmand, "Preparation, characterization and in vitro evaluation of PEGylatednanoliposomal containing etoposide on lung cancer," *Artif Cells NanomedBiotechnol*, vol. 47, no. 1, 2019, doi: 10.1080/21691401.2019.1646265.

[13] S. Jiang, L. Huang, H. Zhen, P. Jin, J. Wang, and Z. Hu, "Carboplatin versus cisplatin in combination with etoposide in the first-line treatment of small cell lung cancer: a pooled analysis," *BMC Cancer*, vol. 21, no. 1, 2021, doi: 10.1186/s12885-021-09034-6.

[14] S. P. Joel *et al.*, "Pharmacological attempts to improve the bioavailability of oral etoposide," *Cancer ChemotherPharmacol*, vol. 37, no. 1–2, 1995, doi: 10.1007/BF00685639.

[15] K. Marigny, F. Aubin, G. Burgot, E. Le Gall, and V. Gandemer, "Particular cutaneous side effects with etoposide-containing courses: Is VP16 or etoposide phosphate responsible?," *Cancer ChemotherPharmacol*, vol. 55, no. 3, 2005, doi: 10.1007/s00280-004-0858-2.

[16] K. R. Hande, "Etoposide: Four decades of development of a topoisomerase II inhibitor," *Eur J Cancer*, vol. 34, no. 10, 1998, doi: 10.1016/S0959-8049(98)00228-7.

[17] T. T. Le *et al.*, "Etoposide promotes DNA loop trapping and barrier formation by topoisomerase II," *Nat Chem Biol*, vol. 19, no. 5, 2023, doi: 10.1038/s41589-022-01235-9.

[18] N. O. Karpinich, M. Tafani, R. J. Rothman, M. A. Russo, and J. L. Farber, "The course of etoposide-induced apoptosis from damage to DNA and p53 activation to mitochondrial release of cytochrome c," *Journal of Biological Chemistry*, vol. 277, no. 19, 2002, doi: 10.1074/jbc.M110629200.

[19] J. M. Fortune and N. Osheroff, "Topoisomerase II as a target for anticancer drugs: When enzymes stop being nice," 2000. doi: 10.1016/s0079-6603(00)64006-0.

[20] J. L. Nitiss, "Targeting DNA topoisomerase II in cancer chemotherapy," 2009. doi: 10.1038/nrc2607.

[21] C. H. Heldin, "Targeting the PDGF signaling pathway in tumor treatment," 2013. doi: 10.1186/1478-811X-11-97.

[22] M. L. Slevin, "The clinical pharmacology of etoposide," *Cancer*, vol. 67, no. 1 S, 1991, doi: 10.1002/1097-0142(19910101)67:1+<319: AID-CNCR2820671319>3.0.CO;2-D.